THE JOURNAL OF PHYSICAL CHEMISTRY A

Article

pubs.acs.org/JPCA

Temperature and Pressure Dependence of the Reaction S + CS (+M) → CS_2 (+M)

Peter Glarborg,[†] Paul Marshall,[‡] and Jürgen Troe*[,§,∥]

[†]Department of Chemical and Biochemical Engineering, Technical University of Denmark, DK-2800 Kongens Lyngby, Denmark

[‡]Department of Chemistry and Center for Advanced Scientific Computing and Modeling (CASCaM), University of North Texas, 1155 Union Circle 305070, Denton, Texas 76203-5017, United States

[§]Institut für Physikalische Chemie, Universität Göttingen, Tammannstrasse 6, D-37077 Göttingen, Germany

[∥]Max-Planck-Institut für Biophysikalische Chemie, Am Fassberg 11, D-37077 Göttingen, Germany

ABSTRACT: Experimental data for the unimolecular decomposition of CS_2 from the literature are analyzed by unimolecular rate theory with the goal of obtaining rate constants for the reverse reaction S + CS (+M) → CS_2 (+M) over wide temperature and pressure ranges. The results constitute an important input for the kinetic modeling of CS_2 oxidation. CS_2 dissociation proceeds as a spin-forbidden process whose detailed properties are still not well understood. The role of the singlet−triplet transition involved is discussed.

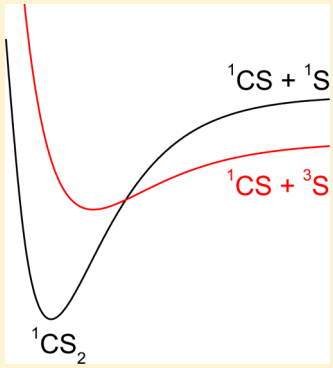

INTRODUCTION

The oxidation of CS_2 leads to a variety of sulfur-containing species by a mechanism that has been the subject of a number of kinetic modeling studies (for a summary of earlier work, see ref 1). As the agreement between measurements and kinetic models leaves a lot to desire, it appears necessary to inspect the rate constants of individual reaction steps and their accuracies in more detail again. One of these reactions is the combination of S atoms with CS,

$$S + CS\ (+M) \rightarrow CS_2\ (+M) \qquad (R-1)$$

It is potentially important[1] as a terminating step in the low-temperature oxidation of CS_2. As there are apparently no direct measurements of the rate of this reaction, one has to rely on experimental data for the reverse thermal decomposition of CS_2,

$$CS_2\ (+M) \rightarrow S + CS\ (+M) \qquad (R1)$$

and convert these with the equilibrium constant

$$K_c = k_1/k_{-1} \qquad (1)$$

This is the issue of the present article. The problem looks easier than it really is. Reaction R−1 first leads into bonding electronically excited triplet states of CS_2 which then undergo triplet−singlet spin inversions into the singlet electronic ground state of CS_2. The detailed dynamics of this mechanism may result in complicated temperature and pressure dependences of the overall rate constants k_1 and k_{-1}. In order to unravel these, help from quantum chemical calculations will be required.

The thermal dissociation of CS_2 (eq R1) has been studied in shock waves since the mid-1960s.[2−8] The results for the low-pressure rate constants $k_{1,0}$ in the bath gas M = Ar are in fair agreement (within about a factor of 3), although the role of the secondary reaction

$$S + CS_2 \rightarrow CS + S_2 \qquad (R2)$$

has been accounted for differently. With the exception of ref 4 the reaction has only been studied under pressure conditions where k_1 was found to be ∝ [Ar], suggesting that the low-pressure limit of the reaction was attained. Increasing the pressure markedly, the transition to the high pressure rate constant $k_{1,\infty}$ could finally be observed in ref 4. (It might be noted that these experiments were quite difficult and ended with the accidental destruction of the apparatus). The low preexponential factor of $k_{1,\infty}$ obtained suggested that reaction R1 indeed proceeds as a spin-forbidden process from singlet electronic ground state CS_2 ($^1\Sigma^+$) through electronically excited triplet states to triplet S (^{3}P) and singlet CS. This appears in agreement with conclusions also drawn from the properties of the measured $k_{1,0}$, such as elaborated later in this article.

Special Issue: 100 Years of Combustion Kinetics at Argonne: A Festschrift for Lawrence B. Harding, Joe V. Michael, and Albert F. Wagner

Received: December 5, 2014
Revised: January 26, 2015
Published: January 27, 2015

DOI: 10.1021/jp5121492
J. Phys. Chem. A 2015, 119, 7277−7281

When k_{-1} is calculated using the equilibrium constant from eq 1 and the data are extended to lower temperatures than applied in the dissociation experiments, the question arises whether reaction R−1 also involves a small energy barrier like the analogous reaction O (^{3}P) + CO (+M) → CO_2 (+M), for which a barrier of about 15.7 kJ mol^{-1} has been suggested in ref 9. The question can be addressed within a general analysis of the value of $k_{1,0}$ in the framework of standard unimolecular rate theory.[10] This approach reveals a number of interesting aspects of the role of the singlet−triplet transition occurring during the process such as discussed in the following.

EXPERIMENTAL LOW-PRESSURE RATE CONSTANTS $k_{1,0}$

Although dissociation experiments could be performed at very high dilution of CS_2 by Ar, the influence of secondary reactions, in particular reaction R2 which under steady-state conditions doubles the rate of CS_2 disappearance, could not always be taken into account properly. Only after k_2 was specified in refs 7 and 11 could this problem be overcome; e.g., apparently the rate constants near 3500 K of ref 3 corresponded to $k_{1,0}$ while those near 2000 K corresponded to $2k_{1,0}$. It appears difficult to give preference to any one of the measured $k_{1,0}$ from refs 2−8 which used a variety of detection methods like UV absorption of the disappearing CS_2 and the forming S (^{3}P) and S (^{1}D) atoms, excited electronic state emission of CS_2, etc. After a proper correction for the influence of reaction R2, here we prefer the data from ref 3, which are close to an average of the rate constants from the low CS_2 concentration experiments of refs 7 and 8 and which cover the largest temperature range. This choice also has the advantage that the pressure dependence can be represented together with the data from ref 4 in an intrinsically consistent manner. Nevertheless, we note the scatter of the various studies by comparing $k_{1,0}$ (2500 K) in Table 1.

Table 1. Experimental Low-Pressure Rate Constants $k_{1,0}$

T, K	$k_{1,0}$(2500 K)/[Ar], cm^3 mol^{-1} s^{-1}	$E_{a,0}/k_B$, K	ref	note[a]
2250−3350	3.1×10^8	41 160	2	a, b
1800−3700	1.7×10^8	42 980	3	a, c, d
1900−3500	2.6×10^8	40 810	5	a, e
2000−2900	0.85×10^8	37 240	6	f
2300−3360	1.2×10^8	38 150	7	g
2200−2900	2.7×10^8	35 480	8	h

[a]Notes: (a) measured rate constant at 2500 K divided by 2; (b) measurements with 0.5% CS_2 in Ar; (c) measurements with 10^{-3}% to (5×10^{-2})% CS_2 in Ar; (d) $E_{a,0}$ reevaluated with variable contributions from reaction R2; (e) measurements with 5% CS_2 in Ar; (f) measurements with 0.2−0.5% CS_2 in Ar, mechanism of secondary reactions accounted for; (g) 5−50 ppm of CS_2 in Ar, reaction R2 chosen similar as in ref 11; (h) 2−10 ppm of CS_2 in Ar, reaction R2 chosen as in ref 11.

The table also includes apparent activation energies $E_{a,0}$ over the given temperature ranges, again after correcting for the influence of reaction R2 in ref 3. In the next section, the measured values of $E_{a,0}$ are analyzed theoretically.

ANALYSIS OF LOW-PRESSURE RATE CONSTANTS $k_{1,0}$

A modeling of $k_{1,0}$ has to take into account the specific features of the spin-forbidden mechanism of the reaction, although the singlet−triplet transition probability only enters the high pressure rate constant $k_{1,\infty}$. Figure 1 illustrates three possible situations. The singlet−triplet transition may lead from the singlet ground state to a repulsive triplet state (curve a) such as the case for the dissociation of N_2O (e.g., see ref 12), to a bonding triplet state with an exit barrier (curve b) as probably the case for the dissociation of CO_2 (e.g., see refs 4 and 9), or to a bonding triplet state without an exit barrier (curve c) such as probably the case for the dissociation of CS_2 considered here; see below. (We note that we consider only one representative, degenerate, triplet state which is most relevant for the reaction; we further neglect electronically excited singlet states.) While the low pressure rate constant in case a is only determined by the properties of the singlet potential and the lowest crossing energy to the repulsive triplet potential, the properties of the bonding triplet state fully contribute in case c as elaborated below.

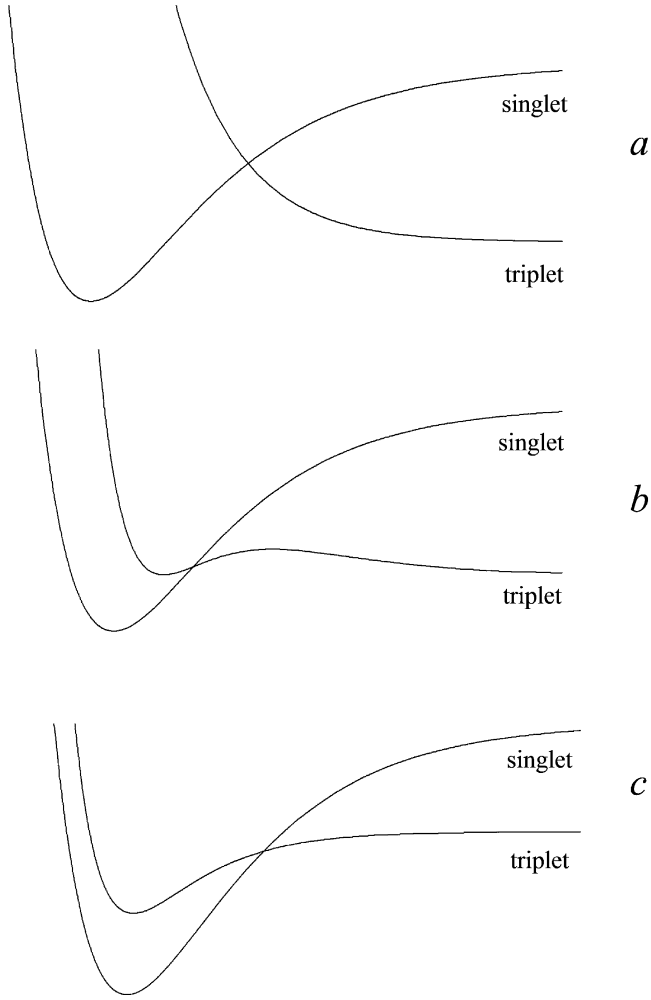

Figure 1. Schematic diagram of crossing potential energy curves in spin-forbidden singlet−triplet dissociation reactions (for cases a, b, and c, see text).

In case b and c situations at low pressures, there is enough time between collisions that the vibrational states in the singlet and triplet near (but slightly below) the triplet dissociation threshold equilibrate between each other. Then the effective vibrational density of states $\rho_{vib}(E_0)$ in the rate constant $k_{1,0}$ includes contributions from the singlet and the triplet, while it corresponds to the singlet only in the case a situation. On the other hand, the effective centrifugal barriers of the reaction, which are also relevant for $k_{1,0}$, differ in the three cases. In case

DOI: 10.1021/jp5121492
J. Phys. Chem. A 2015, 119, 7277−7281

a, these are located near the lowest crossing of the potentials. In case b they are located near the triplet potential maximum. In case c they move to larger interfragment distances governed by the bonding triplet potential. In other words, centrifugal barriers for cases a and b are of rigid character, while they are loose for case c.

We analyze $k_{1,0}$ by the standard formalism of unimolecular rate theory such as formulated in eq 1 of ref 10 (see this reference for the meaning of the various quantities used in the following). With the molecular parameters for the singlet and triplet states of CS_2 given in the Appendix, we obtain $\rho^{S}_{vib,h}(E_0) = 55.8/cm^{-1}$ for the singlet and $\rho^{T}_{vib,h}(E_0) = 10.4/cm^{-1}$ for the triplet states of CS_2 ($^3B_2$). We neglect anharmonicity for the singlet state (because the crossing of singlet and triplet potentials takes place in a still relatively harmonic range of the singlet) but estimate an anharmonicity factor $F_{anh} \approx 2.07$ for the triplet states (which are close to their dissociation limits; see Figure 1). This estimate employs eq 3.8 of ref 13. In addition, we account for the triplet degeneracy such that

$$\rho_{vib}(E_0) \approx \rho^{S}_{vib,h}(E_0) + 3F^{T}_{anh}\rho^{T}_{vib,h}(E_0) \quad (2)$$

leads to $\rho_{vib}(E_0) \approx 120/cm^{-1}$, being about a factor of 2.2 larger than $\rho^{S}_{vib,h}$. We may estimate the rotational factor F_{rot} in the expression for $k_{1,0}$ by its maximum value $F_{rot,max}$ (see eq 15a of ref 10). If F_{rot} would be governed by the crossing of the singlet and the triplet potentials in a case a situation, then, for example, at 2500 K it would be smaller by about a factor of 4. We finally have to estimate the average energy $\langle\Delta E\rangle$ transferred per collision between Ar and excited CS_2. Direct measurements of $\langle\Delta E\rangle$ have been performed by hot UV absorption spectroscopy[14] and IR emission spectroscopy.[15,16] While the former was unable to resolve finer details of the energy dependence of $\langle\Delta E\rangle$ above the triplet excitation energy and led to values as small as $-\langle\Delta E(E_0)\rangle \approx 20\ cm^{-1}$, the better energy resolution of the latter indicated a marked increase of $-\langle\Delta E(E)\rangle$ once the energy of the triplet state of CS_2 was reached. $-\langle\Delta E(E_0)\rangle \approx 100(\pm 50)\ cm^{-1}$ with M = Ar was derived in ref 15. Calculating the collision efficiency β_c with this value, one finally obtains $k_{1,0}$ by the formalism described in ref 10. The value determined for $k_{1,0}(2500\ K)/[Ar] = 1.7 \times 10^8\ cm^3\ mol^{-1}\ s^{-1}$ within the uncertainties of the various input parameters agrees with the experimental results given in Table 1. Assuming a temperature independence of $\langle\Delta E(E_0)\rangle$ in addition, one calculates an apparent activation energy of $E_{a,0}/k_B \approx 42510$ K over the range 2000−3500 K, which is at the upper end of the experimental values shown in Table 1. We do not speculate here about the reasons for minor discrepancies between the various experiments but select the data from ref 3 as being consistent with the modeling. The given analysis provides a first indication that reactions R1 and R−1 do not correspond to a case a but a case c situation in Figure 1. In addition, after having more or less reproduced the experimental values of $k_{1,0}$ at high temperatures by using standard unimolecular rate theory and calculated equilibrium constants, it allows one to extrapolate $k_{1,0}$ and $k_{-1,0}$ to low temperatures. (One should note that a case b situation like for the CO_2 system, with a small triplet barrier that could be of large relevance at low temperatures, cannot be ruled out.)

EXPERIMENTAL HIGH-PRESSURE RATE CONSTANTS $k_{1,\infty}$

While most of the experiments of refs 2, 3, 5−8 were conducted at argon bath gas concentrations below 10^{-5} mol cm^{-3}, the experiments of ref 4 could be extended up to 2×10^{-3} mol cm^{-3}. In this case a transition to a pressure independent rate constant was observed. Deviations from a Lindemann−Hinshelwood falloff curve, on the other hand, could not be detected. However, as the high pressure experiments were difficult to do, broader falloff curves would not have been detectable. The extrapolated high pressure rate constant $k_{1,\infty} \approx 2 \times 10^{-12} \exp(-43780K/T)\ s^{-1}$, as determined over the range 1950−2800 K (assuming fast reaction R10 in contrast to the conclusions from ref 4), at first sight confirms the spin-forbidden character of the reaction. However, before safe conclusions can be drawn, a more detailed analysis of mechanism of the reaction needs to be performed. For a case c potential of Figure 1, the kinetic scheme of eq 3 has to be considered,

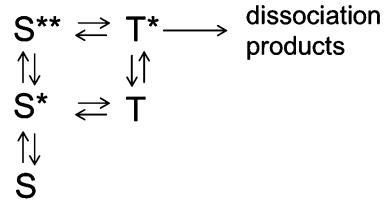

(3)

Here, S denotes vibrational levels of the singlet state of CS_2 and T vibrational levels of the triplet states (as before, we only consider the singlet electronic ground state and a single representative, degenerate, triplet state). S* corresponds to vibrational excitation of S above the minimum crossing energy to the triplet, S** to further vibrational excitation of S up to the dissociation energy of the triplet to S + CS. T* corresponds to vibrational excitation of T up to the latter energy. At low pressures, S* and T as well as S** and T* should have enough time to equilibrate such that the joint collisional vibrational activation of S and T is rate determining as treated in the previous section. At high pressures, collisional vibrational activation and deactivation of S, S*, and S** are fast such that singlet−triplet transitions from S* to T and/or from S** to T* become rate determining. Unlike the case a potential of Figure 1, however, collisional activation and deactivation of T and T* now again are fast such that, besides the process S** → T* → products, the rate of the process S* → T → T* → products is also determined by the singlet−triplet transition from S* to T. This has consequences for the apparent activation energy of $k_{1,\infty}$ as suggested in the following section.

ANALYSIS OF HIGH-PRESSURE RATE CONSTANTS $k_{1,\infty}$

The rate constant $k_{1,\infty}$ for the singlet−triplet transitions S* → T and S** → T* can be represented by[12]

$$k_{1,\infty} = \sum \nu(i^+)\, P(i^+, v)\, f(i^+, v) \quad (4)$$

where i^+ denotes combinations of vibrational quantum numbers that "bring S into contact" with the crossing seam of the singlet and triplet potentials. $\nu(i^+)$ is the frequency of the vibrational mode of the singlet leading to a crossing of the potentials, $P(i^+,v)$ denotes the probability for the transition at the crossing velocity v, and $f(i^+,v)$ is the thermal equilibrium population. According to the quantum chemical calculations of ref 17 (and our own work; see the Appendix), the minimum energy crossing most probably is in bent configuration and its energy is not far from the dissociation energy (at this stage it does not appear possible to decide whether a case b or case c situation is realized). A schematic representation of the bending potentials is shown in Figure 2, as obtained from a CS_2 harmonic bending

DOI: 10.1021/jp5121492
J. Phys. Chem. A 2015, 119, 7277−7281

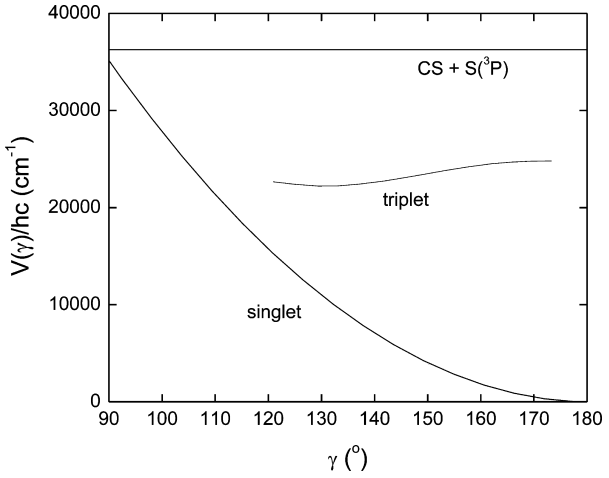

Figure 2. Schematic representation of the angle-dependence of the potential energy surfaces $V(\gamma)$ for the singlet ground state (representation following ref 20) and a representative electronically excited triplet state of CS_2 (see Figure 6 of ref 17).

potential in the singlet ground state and the double-well triplet $^3B_2$ potential from ref 17.

The closeness of the singlet and triplet potentials near their crossing will also allow transitions at energies below the dissociation energy. At high pressures, collisional vibrational activation in the triplet state up to energies above the dissociation energy is fast and will complete the dissociation. As long as collisional activation is not sufficiently fast, the rate of this process will also enter into the rate constant for the rate-determining singlet−triplet transition. Since the two multidimensional potentials are not yet known more precisely, it does not appear worthwhile to model the Airy functional transition probability for all quantum configurations of the singlet leading to the triplet (e.g., see ref 18). Instead, we rationalize the experimental $k_{1,\infty}$ in terms of an expression

$$k_{1,\infty} \approx \nu_{\text{bend}}\, \overline{P_{\text{ST}}}\, \exp\left(\frac{-E_{0,\text{eff}}}{k_{\text{B}}T}\right) \tag{5}$$

with the bending frequency $\nu_{\text{bend}} = 1.2 \times 10^{13}\ \text{s}^{-1}$ of singlet CS_2, a fitted effective average transition probability $\overline{P_{\text{ST}}} \approx {}^1/_6$, and the Boltzmann factor with an effective average singlet−triplet transition energy of $E_{0,\text{eff}} \approx hc\ 30430\ \text{cm}^{-1} = 364\ \text{kJ mol}^{-1}$ (corresponding to the experimental results) being well below the dissociation energy of 435.8 kJ mol^{-1}. This analysis again can be considered consistent with a case c situation in Figure 1. However, the conclusion appears much less certain than that based on the analysis of $k_{1,0}$ given above. (In addition, an extrapolation to low temperatures would appear inadequate if a case b situation would become relevant.)

OVERALL RATE CONSTANTS $k_1([\text{Ar}],T)$ AND $k_{-1}([\text{Ar}],T)$

On the basis of the discussions given before, we consider a low pressure rate constant of

$$k_{1,0}/[\text{Ar}] \approx (5.6 \times 10^{15}) \exp(-42510K/T)\ \text{cm}^3\ \text{mol}^{-1}\ \text{s}^{-1} \tag{6}$$

derived experimentally over the range 1800−3700 K with an uncertainty of about a factor of 2. The less well-known high pressure rate constant according to ref 4 over the range 1900−2800 K amounts to an experimental value of

$$k_{1,\infty} \approx (2 \times 10^{12}) \exp(-43780K/T)\ \text{s}^{-1} \tag{7}$$

At this stage, a Lindemann−Hinshelwood falloff expression

$$k_1/k_{1,\infty} \approx x/(1+x) \tag{8}$$

with $x = k_{1,0}/k_{1,\infty}$ is proposed, since broadening factors $F(x)$ smaller than unity could neither be characterized by experiment nor be characterized by theory; however, they may be there.

The dissociation results can be converted to recombination rate constants for reaction R−1 with equilibrium constants $K_c = k_1/k_{-1}$. On the basis of the molecular parameters summarized in the Appendix, e.g., with the methods of statistical thermodynamics, one calculates

$$K_c = (1.94 \times 10^3) \exp(-56240K/T)\ \text{mol cm}^{-3} \tag{9}$$

over the range 1900−2800 K where low and high pressure experimental data are available. Employing eqs 6−9 then leads to recombination rate constants over the same temperature range. Using the theoretical analysis for low pressure rate constants given above, the derived $k_{-1,0}$ can be extrapolated to lower temperatures (neglecting the possibility of small barriers for a case b situation). The results then are represented as

$$k_{-1,0} \approx (3.4 \times 10^{16})(T/1000K)^{-2.42}\ \text{cm}^6\ \text{mol}^{-2}\ \text{s}^{-1} \tag{10}$$

over the range 300−2000 K. High pressure recombination rate constants are expressed as

$$k_{-1,\infty} \approx (2.4 \times 10^{13})(T/1000K)^{-4.3}\ \text{cm}^3\ \text{mol}^{-1}\ \text{s}^{-1} \tag{11}$$

over the range 1900−2800 K, the latter values being much less certain than $k_{-1,0}$ (and more difficult to extrapolate to lower temperatures). Falloff expressions for k_{-1} are analogous to those for k_1.

Two remarks on the recombination rate constants for reaction R−1 appear necessary. For the analogous recombination reaction O + CO → CO_2 a small activation barrier could clearly be identified.[9] This barrier superimposes a positive temperature coefficient on the negative temperature dependence analogous to that given for $k_{-1,0}$. As a consequence, the recombination O + CO → CO_2 at low temperature is very slow. One might argue that a similar behavior could be present for S + CS → CS_2. However, the presence of such a "rigid" barrier would have introduced a rotational factor F_{rot} markedly below the maximum factor $F_{\text{rot,max}}$ employed above. The agreement between measured and modeled $k_{1,0}$ then would have been destroyed. Therefore, we do not see evidence for such a barrier here and, therefore, conclude that the system corresponds to a case c situation. In any case, $k_{-1,0}$ as given above should be an upper limit. Second, usually the transition between low pressure and high pressure range with decreasing temperature shifts markedly toward lower bath gas concentrations. This is not the case here because $k_{-1,\infty}$ seems to have a stronger temperature dependence than $k_{-1,0}$. However, this conclusion at this stage is only tentative.

One finally may ask why the apparent activation energies of k_1 are so much smaller than the bond energy ($E_0/k_{\text{B}} \approx 52400$ at 0 K). For the low pressure limit, this is just what is explained by standard unimolecular rate theory.[10] As the modeling for the high pressure rate constant cannot yet be done in similar detail as for N_2O dissociation,[12] it has to be remembered that spin-forbidden processes require a specific treatment. In the present

DOI: 10.1021/jp5121492
J. Phys. Chem. A 2015, 119, 7277−7281

case probably more than one triplet state contribute to the reaction. In addition, it is not clear whether the energetically lowest spin-inversion S* → T or the higher inversion step S** → T* dominate the reaction rate. An explanation for the measured low apparent activation energy of eq 7 and the predicted strong temperature dependence of eq 11 may be found at this place. Therefore, further quantum chemical calculations of the structures of the electronically excited triplet states of CS_2 appear necessary. Nevertheless, one may conclude that the present analysis of the measured rate constants appears most consistent with a case c mechanism of Figure 1.

APPENDIX

Molecular parameters used in the modeling (data from ref 19 unless noted otherwise) are as follows:

CS_2 ($^1\Sigma_g^+$): ν_i/cm^{-1} = 657.98, 355.93(2), 1535.35; B/cm^{-1} = 0.1093; σ = 2; $\Delta H_{f,0}^{\circ}$(0 K) = 116.13 kJ mol^{-1}.

CS_2 ($^3B_2$): ν_i/cm^{-1} = 805, 279, 987; B_2/cm^{-1} = 0.121, 0.126, 2.78; $\Delta H_{f,0}^{\circ}$(0 K) = 376.4 kJ mol^{-1} (calculations from this work at the CCSD(T)/aug-cc-pV(T+d)Z level of theory; see also the calculations of ref 17).

CS ($^1\Sigma^+$): ν_i/cm^{-1} = 1285.08; B/cm^{-1} = 0.820046; σ = 1; $\Delta H_{f,0}^{\circ}$(0 K) = 277.1 kJ mol^{-1}.

S (^3P): $\Delta H_{f,0}^{\circ}$(0 K) = 274.73 kJ mol^{-1}. $^3P_2$: 0 (g = 5). $^3P_1$: 396.09 cm^{-1} (g = 3). $^3P_0$: 573.65 cm^{-1} (g = 1).

AUTHOR INFORMATION

Corresponding Author

*E-mail: shoff@gwdg.de.

Notes

The authors declare no competing financial interest.

ACKNOWLEDGMENTS

P.M. thanks the R. A. Welch Foundation (Grant B-1174) for support.

REFERENCES

(1) Glarborg, P.; Halaburt, B.; Marshall, P.; Guillory, A.; Troe, J.; Thellefsen, M.; Christensen, K. Oxidation of Reduced Sulfur Species: Carbon Disulfide. *J. Phys. Chem. A* **2014**, *118*, 6798−6809.

(2) Gaydon, A. G.; Kimbell, G. H.; Palmer, H. B. Shock-Tube Study of Kinetics of Decomposition of Carbon Disulphide. *Proc. R. Soc. London* **1964**, *279*, 313−326.

(3) Olschewski, H. A.; Troe, J.; Wagner, H. Gg. Unimolekularer Zerfall von CS_2 in Stosswellen. *Z. Phys. Chem.* **1965**, *45*, 329−338.

(4) Olschewski, H. A.; Troe, J.; Wagner, H. Gg. Untersuchung Unimolekularer Reaktionen bei Hohen Drucken in Stosswellen. *Ber. Bunsenges. Phys. Chem.* **1966**, *70*, 1060−1064.

(5) Arnold, S. J.; Brownlee, W. G.; Kimbell, G. H. Reactions of Shock-Heated Carbon Disulfide-Argon Mixtures. II. Kinetics of the Dissociation of Carbon Disulfide. *J. Phys. Chem.* **1970**, *74*, 8−14.

(6) Saito, K.; Toriyama, Y.; Yokubo, T.; Higashikava, T.; Murakami, I. A Measurement of the Thermal Decomposition of CS_2 behind Reflected Shock-Waves. *Bull. Chem. Soc. Jpn.* **1980**, *53*, 1437−1438.

(7) Woiki, D.; Roth, P. A Shock Tube Study on the Thermal Decomposition of CS_2 Based on S(^{3}P) and S(^{1}D) Concentration Measurements. *Shock Waves* **1994**, *4*, 95−99.

(8) Murakami, Y.; Kosugi, M.; Susa, K.; Kobayashi, T.; Fujii, N. Kinetics and Mechanism for the Oxidation of CS_2 and COS at High Temperature. *Bull. Chem. Soc. Jpn.* **2001**, *74*, 1233−1240.

(9) Troe, J. Atom and Radical Recombination Reactions. *Annu. Rev. Phys. Chem.* **1978**, *29*, 223−250.

(10) Troe, J. Predictive Possibilities of Unimolecular Rate Theory. *J. Phys. Chem.* **1979**, *83*, 114−126.

(11) Homann, K. H.; Krome, G.; Wagner, H. Gg. Carbon Disulfide Oxidation. 3. Isothermic Oxidation of Carbon Disulfide. *Ber. Bunsenges. Phys. Chem.* **1970**, *74*, 654−659.

(12) Olschewski, H. A.; Troe, J.; Wagner, H. Gg. Niederdruckbereich und Hochdruckbereich des Unimolekularen N_2O-Zerfalls. *Ber. Bunsenges. Phys. Chem.* **1966**, *70*, 450−459.

(13) Troe, J. Simplified Models for Anharmonic Numbers and Densities of Vibrational States. 1. Application to NO_2 and H_3^+. *Chem. Phys.* **1995**, *190*, 381−392.

(14) Dove, J. E.; Hippler, H.; Troe, J. Direct Studies of Energy Transfer of Vibrationally Highly excited CS_2 Molecules. *J. Chem. Phys.* **1985**, *82*, 1907−1919.

(15) Hartland, G. V.; Qin, D.; Dai, H. L. Intramolecular Electronic Coupling Enhanced Collisional Deactivation of Highly Vibrationally Excited Molecules. *J. Chem. Phys.* **1995**, *102*, 8677−8680.

(16) Chimbayo, A.; Toselli, B. M.; Barker, J. R. Deactivation of Highly Vibrationally Excited CS_2 and SO_2 by Rare Gases. *J. Chem. Phys.* **1998**, *108*, 2383−2394.

(17) Brown, S. T.; van Huis, T. J.; Hoffman, B. C.; Schaefer, H. F., III. Excited Electronic States of CS_2. *Mol. Phys.* **1999**, *96*, 693−704.

(18) Troe, J.; Wagner, H. Gg. Unimolecular Reactions in Thermal Systems. *Ber. Bunsenges. Phys. Chem.* **1967**, *71*, 937−979.

(19) *NIST-JANAF Thermochemical Tables*; Chase, M. W., Ed.; Journal of Physical and Chemical Reference Data, Monograph No. 9; American Institute of Physics: Woodbury, NY, 1998.

(20) Herzberg, G. *Molecular Spectra and Molecular Structure. II. Infrared and Raman Spectra of Polyatomic Molecules*; Van Nostrand: New York, 1945.

DOI: 10.1021/jp5121492
J. Phys. Chem. A 2015, 119, 7277−7281